NUMERICAL MODELLING OF SURFZONE RETENTION IN RIP CURRENT SYSTEMS: ON THE IMPACT OF THE SURFZONE SANDBAR MORPHOLOGY

Bruno Castelle[1], Ad Reniers[2] and Jamie MacMahan[3]

Abstract

Simulations from a numerical model address the impact of surfzone sandbar morphology on surfzone retention on open rip-channeled beaches exposed to shore-normal waves. Rip channels are regularly spaced alongshore with a given wavelength λ. For a given reference case bathymetry (λ = 200 m) loosely based on existing field observations of rip channels, rip current circulations retain floating material (simulated using passive drifters) at a hourly rate of about 80% which is in line with existing field and laboratory studies. The influence on surf zone retention is evaluated by five morphologic parameters: 1) the vertical amplitude of the alongshore-uniform sandbar, 2) the horn and bay sequence, 3) rip head bar and 4) the ratio of the alongshore length of the shoal to that of the channel and 5) rip spacing. Results show that rip channel spacing is the most important parameter, with surfzone retention decreasing with increasing rip spacing. The ratio of the surf zone Xs width to rip spacing λ controls surfzone retention. The surfzone retention increases with Xs/λ up to a threshold, with mean rip current intensity showing the opposite trend. These results suggest that both the underlying nearshore bathymetry and an accurate estimation of the surfzone width and rip channel spacing must be taken into account to further improve our ability to understand and predict surfzone retention on open rip-channeled beaches which is important to beach safety and horizontal water mixing.

Key words: Rip current, surfzone retention, numerical modeling, rip spacing, surfzone width, drifters

1. Introduction

Rip currents (Figure 1; MacMahan *et al*., 2006; Dalrymple *et al*., 2011) are powerful, channeled seaward flowing currents of water that are ubiquitous along wave-dominated sandy beaches that exhibit three-dimensional surfzone sandbars (*i.e*. rip channels and crescentic patterns). They are one of the most deadly coastal hazards (Scott *et al*., 2011) and are important to transport and dispersion of pollutants, nutrients and tracers (Shanks *et al*., 2010) and to short-term (from days to weeks) sandy beach morphodynamics (*e.g*., Castelle and Ruessink, 2011). On rip channeled-beaches, rip currents are driven by alongshore variations in depth-induced wave breaking dissipation due to the alongshore variability in depth of the surfzone sandbar (Bonneton *et al*., 2010). Rip velocity typically fluctuates on timescales of the order of 1 minute (infragravity motions; *e.g*. MacMahan *et al*., 2004a) and 10 minutes (Very Low Frequency motions, VLFs; *e.g*. MacMahan *et al*., 2004b).

The accepted view of rip currents was that they are an efficient mechanism for transporting material out of the surf zone. Recent field (MacMahan *et al*., 2010), numerical (Reniers *et al*., 2009) and laboratory (Castelle *et al*., 2010) studies challenged this traditional paradigm. Rip current circulation patterns actually most of the time consist of semi-enclosed vortices that retain floating material within the vortex center and remain within the surf zone. Approximately 10-20% of the drifters deployed in the rip currents exit the surf zone per hour on average during the numerical and field experiments. Using attractive Lagrangian Coherent Structures (LCS, Shadden *et al*., 2005) hidden in the pulsating rip-current surface velocity field, Reniers *et al*. (2010) show that the primary exit mechanism of floating material in rip current circulation is associated with VLF dynamics and the resulting eddies that detach from the main rip current (Reniers *et al*., 2010).

[1]UMR EPOC, Université Bordeaux I, Avenue des Facultés, Talence 33405, France. b.castelle@epoc.ubordeaux1.fr
[2]Rosenstiel School of Marine and Atmospheric Science, University of Miami, Miami, FL 33149, USA. areniers@rsmas.miami.edu
[3]Oceanography Department, Naval Postgraduate School, Monterey, CA 93943,USA. jhmacmah@nps.edu

Figure 1. Rip current extending beyond the surf zone at Collaroy Beach (Australia). The rip current is identified by the sediment plume.

Yet, during the DRIBS2 experiment at Perranporth (UK) much higher rates of drifter exits were sometimes measured (Austin *et al*., 2013). This was further confirmed by recent observations on Australian rip-channeled beaches (McCarroll *et al*., 2013). In addition, in the laboratory Castelle *et al*. (2011) measured drifter exit rates ranging from about 5% to 45% (with a mean of 20%) for the same normal-incidence wave conditions, but different surfzone sandbar morphologies. This suggests a control of the nearshore morphology on surfzone retention rates. This control, which is poorly understood, is addressed in this contribution. A coupled wave-circulation model (Section 2) is used to examine the role of surfzone sandbar morphology on surfzone retention (Section 3) followed by a discussion on the significance of the morphological parameters in Section 4.

2. Model

2.1. *XBeach*

The open source model XBeach (Roelvink *et al*., 2009) is used herein, which is the Eastern 2012 version, that solves coupled 2D horizontal equations for wave propagation, flow, sediment transport and bottom changes, switching off the latter in this contribution. XBeach includes the wave-group forced VLFs and solves the Generalized Lagrangian Mean (GLM) flow velocity as both must be accounted for to accurately simulate surfzone retention on natural rip-channel beaches (Reniers *et al*., 2009). Wave-current interaction is taken into account in our computations. To identify the preferred pathways of surf zone exits and trapping zones of floating matter, Finite-Time Lyapunov Exponent (FTLE) fields are computed, whose maximizing ridges represent the LCSs (Shadden *et al*., 2005). The FTLE is estimated with a time integration interval τ = -10 min to focus on LCS of attracting type on the timescales of VLF flow dynamics (Reniers *et al*., 2010).

2.2. *Model set-up*

2.2.1. *Bathymetries and wave conditions*

The beach extends 2000 m and 700 m in the longshore (x axis) and cross-shore (y axis) direction, respectively, with a regular grid spacing of 5 m in both directions. The model is run for a number of different bathymetries characterized by contrasting surfzone sandbar morphologies (Figure 2). A given rip-channeled beach is generated starting from a 1:50 planar sloping seabed profile with the offshore boundary at 11.5 m depth with a superimposed alongshore-uniform sandbar located 100 m from the shoreline with a vertical amplitude *Hb* (Figure 2a). Bar and rip patterns are superimposed as an alongshore sequence of horns and bays alternating shoreward of the bar crest with a wavelength λ and a vertical amplitude *A* (Figure 2b). In Figure 2b horns and bays have the same alongshore length (namely *S* = 1). Patterns with different horn to bay alongshore ratios (*S* = 2 and 3) are generated to account for the commonly observed rip channel narrowness with respect to the shoal (*e.g*. Brander, 1999; Bruneau *et al*., 2011). In addition, for some simulations we superimposed a rip head bar system (Brander, 1999) as an alongshore sequence of horns and bays alternating seaward of the bar crest (with the same wavelength λ and out of phase with respect to the shoreward sequence, see Figure 2b) with a vertical amplitude *Arhb*. Hereafter the bathymetry with λ = 200 m, *S* = 1, *A* = 1.5 m, *Arhb* = 0 and *Hb* = 0.5 m is referred to as the reference case simulation. For all the other bathymetries, only one parameter is varied and all the others are kept the same as in the reference case simulation.

For all the simulations, shore-normal wave forcing is applied at the offshore boundary with a significant wave height *Hs* = 1.5 m, a peak wave period *Tp* = 10 s. Wave groups are generated using a parametric Jonswap spectrum with a peak enhancement factor of 3.3 and a directional spreading of 10° using the cosine law. Simulations last 1.5 hours but to prevent initial transient effects the first 30 minutes (-30 min < *t* < 0) are ignored and results are analyzed for 0 < *t* < 60 min.

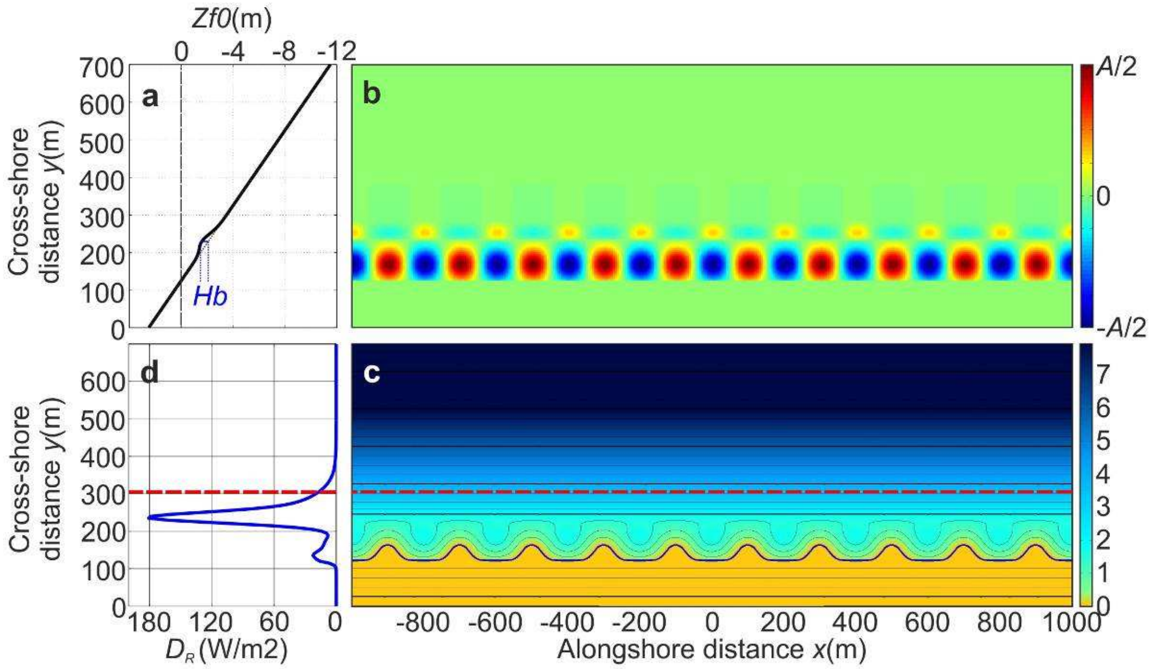

Figure 2. Set-up of a nearshore bathymetry with (a) an alongshore-uniform single-barred beach profile (with *Hb* the bar amplitude) with (b) a superimposed horn and bay sequence with a vertical amplitude *A* and an alongshore spacing λ resulting in (c) a rip-channeled beach (colorbar indicates still water depth in meters) with the red dotted line indicating the offshore extent of the surf zone compartment computed in (d) as the location where the alongshore-averaged cross-shore roller energy D_R exceeds 10% of its cross-shore maximum (Reniers *et al*., 2009). In (c) and (d) results are given for the reference case simulation (λ = 200 m, *S* = 1, *A* = 1.5 m, *Arhb* = 0, *Hb* = 0.5 m) except that in (b) the location of the rip-head-bar horn/bay sequence (with *Arhb* << *A*) is also indicated.

2.2.2. *Surfzone retention computations*

For each simulation, passive drifters are initially (t = 0) uniformly seeded at 2-m intervals in the inner surf zone at -500 m < x < 500 m to prevent edge effects due to the Neumann lateral boundary conditions. Drifter trajectories are then calculated at each time step (equal to 1 s) using GLM velocities. The outer edge of the surf zone compartment (Figure 2c) is defined as the location where the alongshore-averaged cross-shore roller energy exceeds 10% of its cross-shore maximum (Reniers *et al*., 2009; see Figure 2d). Hourly retention rate R is then computed as the number of drifters within the surf zone compartment at the end of the simulation expressed as the percentage of the total number of active drifters initially seeded.

3. Results

3.1 *Reference case simulation*

The time evolution of drifter positions and LCSs for the reference case simulation (λ = 200 m, S = 1, A = 1.5 m, $Arhb$ = 0, Hb = 0.5 m) are shown in Figure 3. Consistent with a previous study (Reniers *et al*., 2009), the initially uniformly distributed drifters rapidly converge along the LCSs associated with VLFs dynamics (*e.g*., Figures 3b, c and d). A small number of exits from the surf zone are observed with most exits occurring in the alignment of the rip channels. Drifters entering a rip current tend to recirculate within the eddy associated with the rip current system. The rip current flow field, consisting of semi-enclosed large-scale vortices that retain the drifters, is consistent with Lagrangian observations on rip-channeled beaches in both the field (MacMahan *et al*., 2010) and the laboratory (Castelle *et al*., 2010). Only a small number of drifters pass from one rip current system to another (see for instance the small number of drifters observed at x > 500 m and x < -500 m by the end of the simulation, Figure 3g). This suggests a rather small interchange of water between the nearby rip current systems, which is once again in line with drifter behavior on rip-channeled beaches exposed to shore-normal waves (*e.g*., Castelle *et al*., 2010). The hourly surfzone retention rate for this simulation is 81.15%, which is similar to that typically found along rip-channeled open beaches (MacMahan *et al*., 2010).

For this simulation, classic mean rip current patterns are observed (Figure 4a) with alongshore feeder currents, a reasonably intense (~0.7-0.8 m/s) and narrow offshore-directed jet in the channel, strong onshore-directed flow across the shoals and counter rotating cells to the left and right of the rip current. Drifter exits occur in the alignment of the rip channel (yellow arrow in Figure 4a).

3.2. *Impact of surfzone sandbar morphology*

The surfzone retention results obtained for different nearshore sandbar morphologies are summarized in Table 1. Results show that the vertical amplitude of both the alongshore-uniform sandbar (Hb) and the horn and bay sequence (A) do not impact significantly surfzone retention as hourly rates of about 80% are systematically observed when varying one of these 2 parameters. The influence of the presence of a rip head bar ($Arhb$) or a varying ratio of the alongshore lengths of the horns (S) and bay is less clear: (1) varying S results in R ranging from 80 to 90% with no general trend and (2) increasing the rip head bar vertical amplitude does not impact R (*i.e*., R = 82.9% for S = 2, Table 1) up to a certain threshold above which R drastically decreases (R = 59.89% for S = 3, Table 1). The role of the rip head bar on surfzone retention and mean rip current circulation will be discussed later in this paper.

Changing rip spacing λ impacts significantly hourly surfzone retention rate with R readily increasing with decreasing λ (Table 1). For instance, R drops to 45.36% for λ = 400 m, which is very low compared with existing field and laboratory observations. In contrast, for rip channels regularly spaced at a narrow wavelength λ = 100 m, R exceeds 90% revealing a very low rate of surfzone flushing. Interestingly, mean rip current intensity $Urip$ increases with increasing retention R when varying λ.

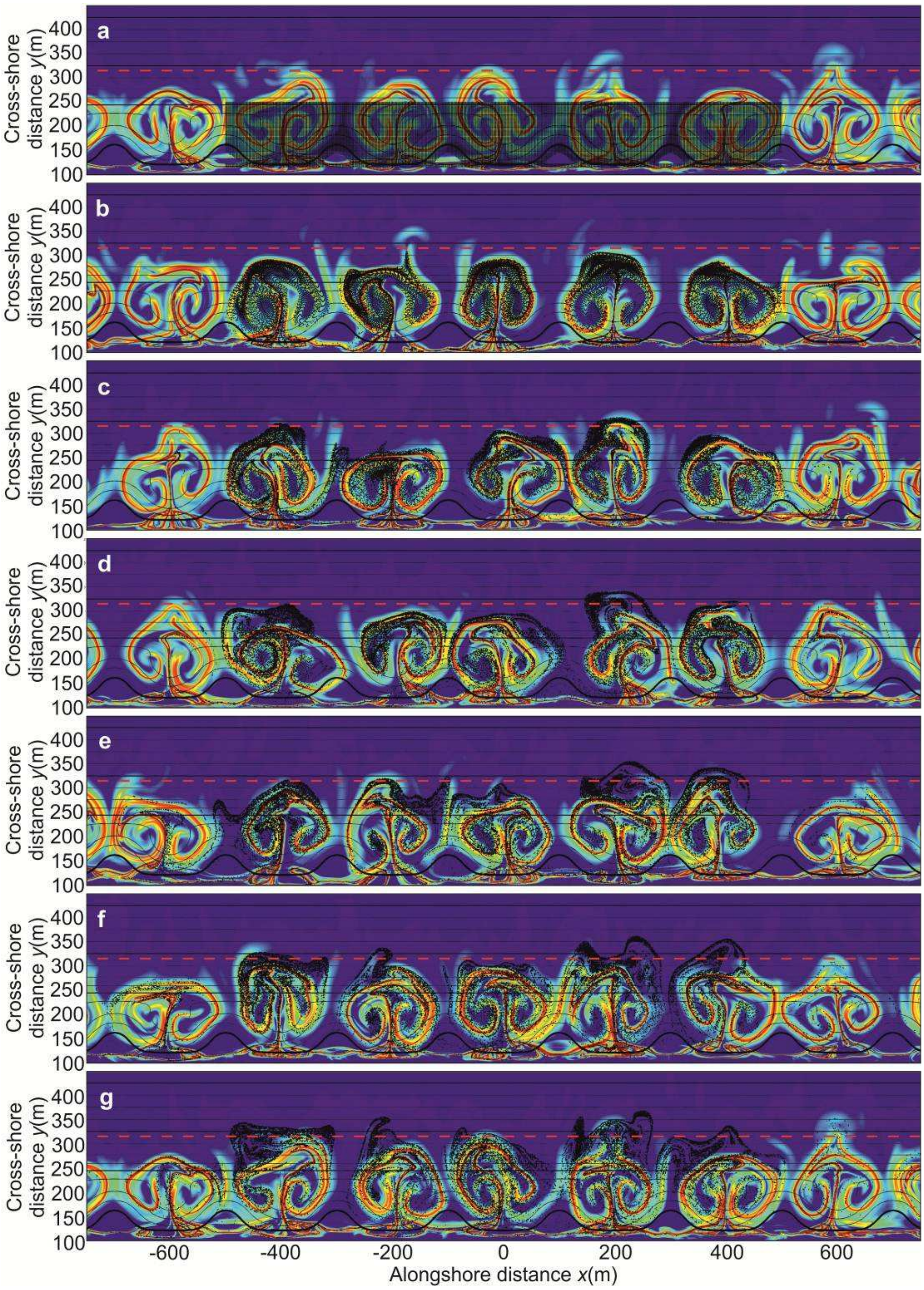

Figure 3. Snapshots (zoom at -750 m < x < 750 m and 100 < y < 450 m) of backward-time ($\tau = -10$ min) FTLE field (red curves represent the LCSs) and computed drifter positions (black dots) for the reference case simulation (a) 0, (b) 10, (c) 20, (d) 30, (e) 40, (f) 50 and (f) 60 minutes after virtual drifter (black dots) seeding in the surf zone. Iso-contours (0.5-m intervals) are contoured in the background, the dashed red line and thick black line indicates the edge of the surf zone compartment and the shoreline, respectively. Time evolution shows that initially uniformly distributed drifters rapidly converge along the LCSs associated with VLFs dynamics forming narrow streaks with a small number of exits from the surf zone compartment.

Table 1. Table summarizing surfzone retention results for different nearshore sandbar morphologies. The reference case simulation is shown in bold red, and the 3 simulations further discussed in Figure 5 are shown in bold black.

λ (m)	*S*	*A* (m)	*Arhb* (m)	*Hb* (m)	*Urip* (m/s)	*R* (%)
200	**1**	**1.5**	**0.**	**0.5**	**0.768**	**81.15**
200	2	1.5	0.	0.5	0.770	91.20
200	3	1.5	0.	0.5	0.767	81.06
200	1	1.0	0.	0.5	0.636	86.11
200	1	2.0	0.	0.5	0.909	81.61
200	1	1.5	0.2	0.5	0.802	82.90
200	**1**	**1.5**	**0.4**	**0.5**	**0.919**	**59.89**
200	1	1.5	0.	0.	0.880	83.39
200	1	1.5	0.	1.0	0.701	80.18
100	**1**	**1.5**	**0.**	**0.5**	**0.596**	**90.35**
400	**1**	**1.5**	**0.**	**0.5**	**0.776**	**45.36**

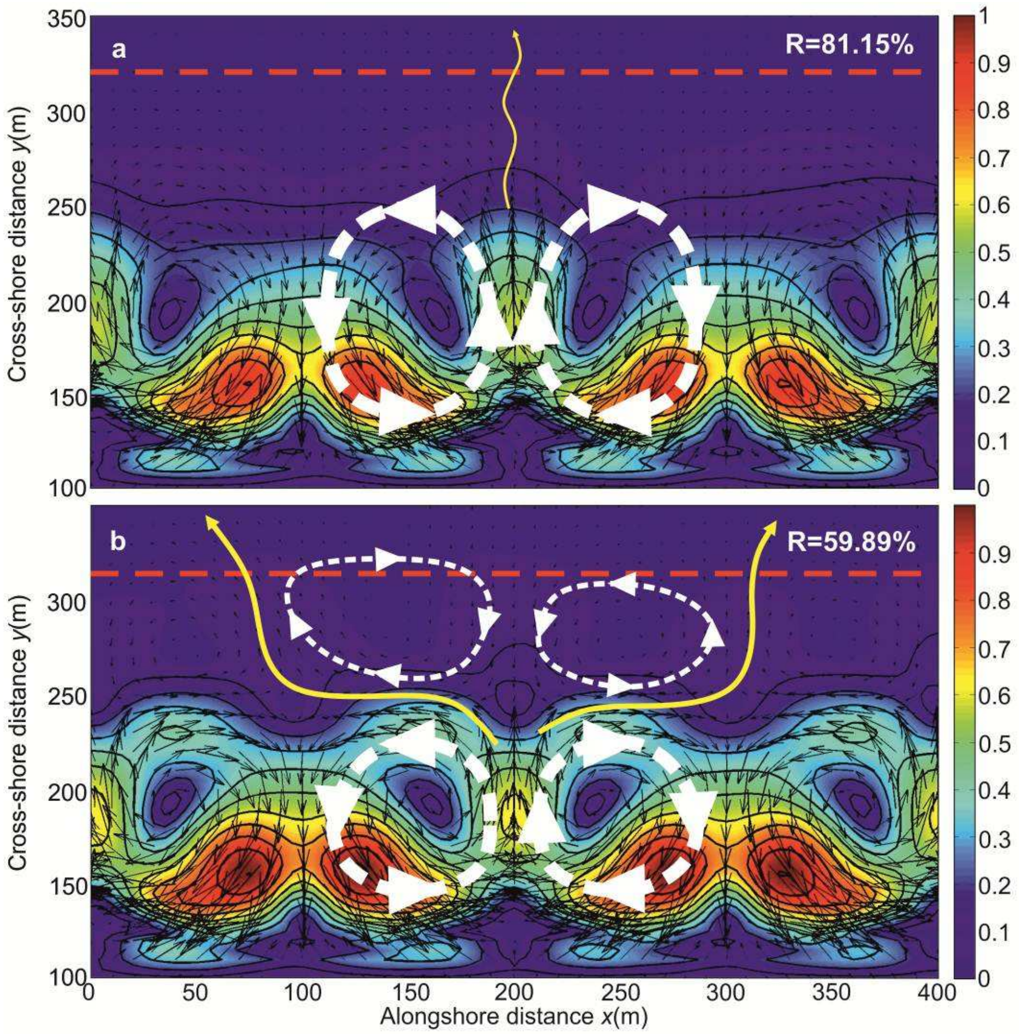

Figure 4.Computed mean flow patterns (for clarity one out of two vectors are plotted in both directions) and surfzone retention *R*. Colorbar indicates mean flow velocity in m/s. The dotted white circles and yellow arrows indicate qualitatively the surf zone eddies and the preferred pathways of drifter exits. (a) Reference case simulation and (b) simulation with the presence of a well-developed rip head bar with *Arhb* = 0.4 m.

Snapshots of drifter positions (black dots) at t = 60 min and resulting hourly retention rate R are shown in Figure 5 (with the reference case simulation in Figure 5a). When a well-developed rip head bar system is considered ($Arhb$ = 0.4, Figure 5b) surf zone flushes out a lot of floating material with a computed hourly retention rate of 59.89%. In contrast with the reference case simulation, drifters exit the surf zone preferably in the alignment of the shoals. In addition, drifters are expulsed further offshore than in all the other simulations as a large number of drifters are found at y > 350 m (see the mushroom shape clusters of drifters in Figure 5b). In this situation, intense depth-induced wave breaking is observed across the rip head bars. This in turn drives a, counter rotating, more seaward circulation in which drifter exits occur through the, weak (<0.1 m/s, Figure 4b), offshore-directed flow.

For λ = 100 m (Figure 5c), R > 90% as most of the drifters remain within the surfzone compartment. By the end of the simulation, a significant number of drifters are located within the semi-enclosed large-scale vortices that display both alongshore and cross-shore shorter scales. Even if a large number of drifters actually exited the semi-enclosed vortices, most of them do not reach the offshore limit of the surfzone compartment located at y = 315 m (Figure 5c), resulting in a high surfzone retention. This contrasts with the situation with λ = 400 m (Figure 5d) in which both the alongshore and cross-shore scales of the large-scale vortices are much larger. This results in a large number of drifters exiting the surfzone compartment, with a low hourly surfzone retention rate R = 45.36%. Accordingly, from our simulations rip spacing λ appears to be an important parameter controlling surfzone retention. For a given offshore wave height (and consequently a given surfzone width Xs), rip channel spacing impacts the cross-shore length of the large-scale vortices with its offshore extent moving closer to the outer edge of the surf zone with increasing λ. The relationship between R, λ and Xs is further discussed next.

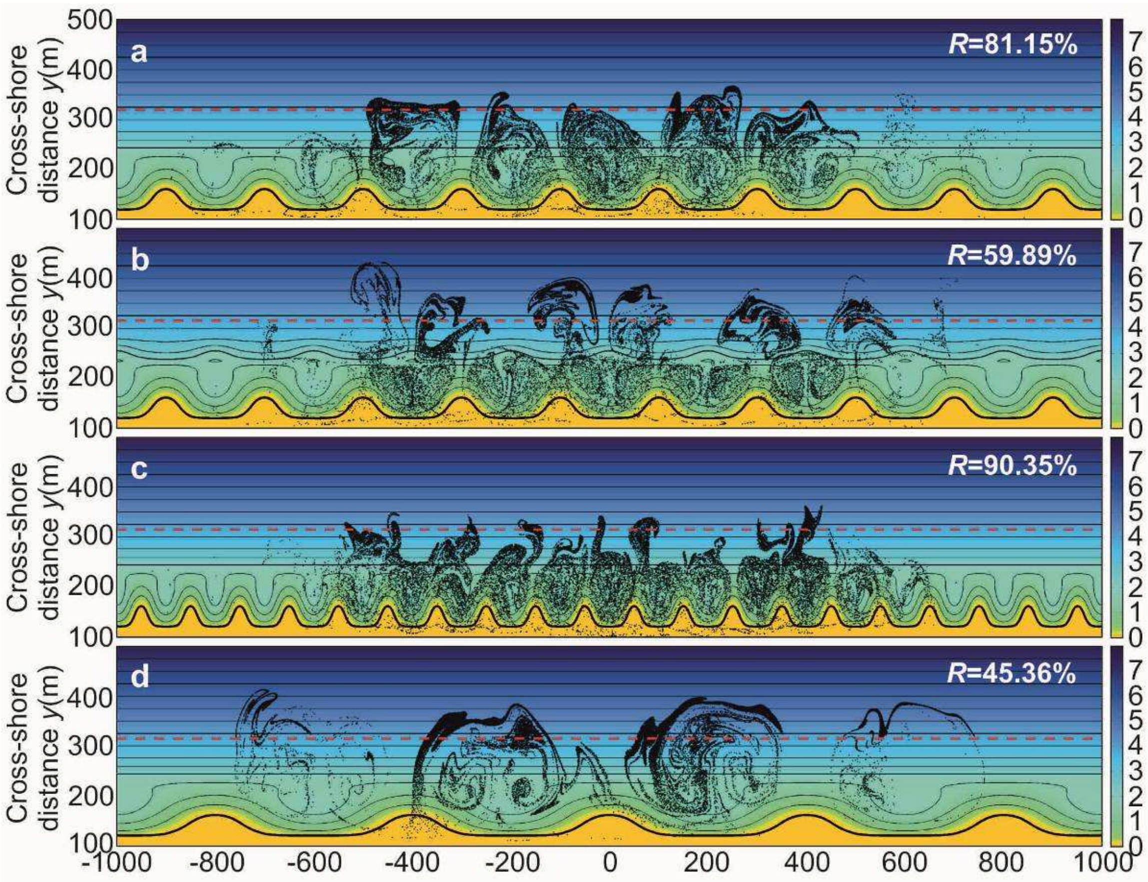

Figure 5. Snapshot of drifter positions (black dots) at t = 60 min and resulting hourly retention rate R for (a) the reference case simulation (b) adding a rip head bar with $Arhd$ = 0.4 m and with different spacings (c) λ = 100 m and (d) λ = 400 m. In all panels, surf zone compartment is indicated by the dashed red line and iso-contours (0.5-m intervals) are contoured in the background. Colorbars indicate still water depth in meters.

4. Discussion and conclusions

Most of the simulations indicate an hourly surfzone retention rate of about 80%, which is in line with recent studies on surfzone retention (*e.g*., Reniers *et al*., 2009; MacMahan *et al*., 2010; Castelle *et al*., 2011). Once again in line with previous works (Reniers et al., 2010), the primary exit mechanism of floating material in our simulated rip current circulation is associated with VLF dynamics and the resulting eddies that detach from the main rip current (see LCS of attracting type on the timescales of VLF flow dynamics in Figure 3). Quite surprisingly, most of the sandbar morphology parameters tested do not impact significantly surfzone retention rate. Instead, for a given surfzone width *Xs*, only the impact of rip spacing λ on surfzone retention is clear.
Additional simulations are run varying λ from 50 m to 500 m (every 25 m) to further explore the role of rip spacing on surfzone retention. The non-dimensional parameter $\delta = Xs/\lambda$ is computed, which represents a measure of the alongshore constraint of the large-scale vortices associated with the rip current. Figure 6 shows both *R* and mean rip current velocity *Urip* versus δ. Corroborating earlier findings, surfzone retention increases with increasing δ up to the threshold $\delta \approx 1.2$. For $\delta > 1.2$ surfzone retention is systematically about 90%, corresponding to situations when the surfzone width is substantially larger than rip spacing. In contrast, rip current velocity decreases with increasing δ for $\delta > 0.7$. This means that surfzone retention rate roughly shows the opposite trend to that of rip current velocity when varying δ.

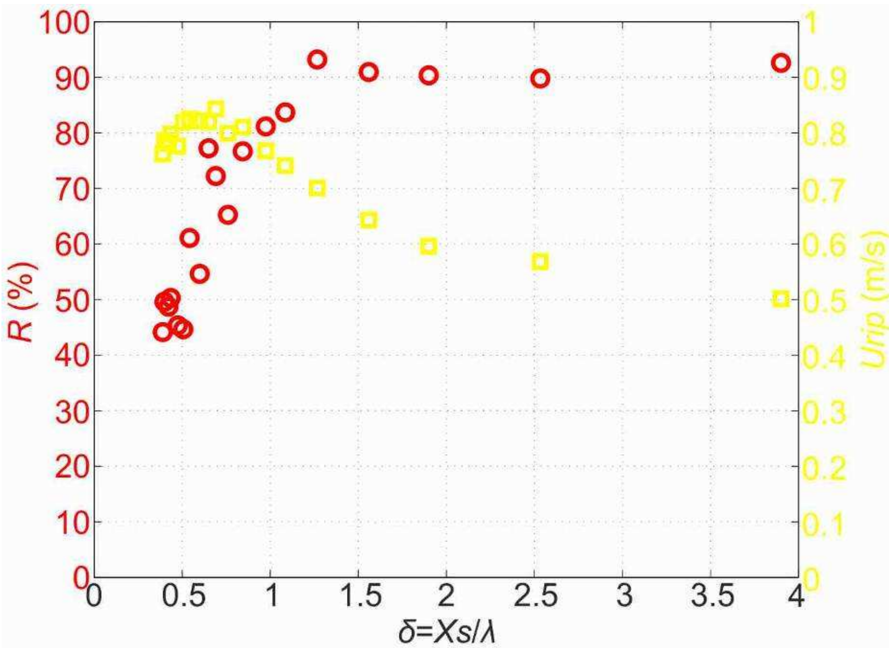

Figure 6. Hourly surfzone retention rate *R* and rip current intensity *Urip* versus the non-dimensional parameter $\delta=Xs/\lambda$ for rip-channeled beaches with the same morphological characteristics but varying λ from 50 m to 500 m every 25 m.

Overall, the results indicate that, on single-barred rip-channeled beaches, the surfzone width *Xs* and rip spacing λ controls surfzone retention rate with *R* increasing with increasing $\delta=Xs/\lambda$. This must be further explored with varying the offshore wave height as here δ was varied only addressing changes in rip spacing λ. The influence of wave obliquity must also be further tested. In addition, for each configuration a larger number (*e.g*. 10) will have to be performed to filter the sensitivity of *R* to a given, time-varying, wave-group series.
These results presumably do not apply to other types of rips commonly found on wave-exposed coast that is, when rip currents are not driven by alongshore variations in depth-induced wave breaking dissipation due to the alongshore variability in depth of the surfzone sandbar. For instance, surf zone flushing is likely much more relevant on alongshore-uniform beaches where flash rips (*e.g*. Dalrymple, 1975; Johnson and

Pattiaratchi, 2004; Murray *et al*., 2013), rips driven by the presence of an offshore bathymetric anomaly (*e.g*. Long *et al*., 2005), or headland rips (*e.g*. Short, 2007; Castelle *et al*., in press) occur. In addition, in multiple-barred beaches, the morphology of an outer bar likely influences surf zone exits (*e.g*. Austin et al., 2013). These numerical results presented stimulate future detailed field observations and numerical studies of surfzone retention to further test this hypothesis and to improve our ability to predict surfzone flushing on open beaches.

Acknowledgements

This work was done within the framework of the project BARBEC (ANR N2010 JCJC 602 01).

References

Austin, M.J., Scott, T.M., Russell, P.E. and Masselink, G., 2013. Rip Current Prediction: Development, Validation, and Evaluation of an Operational Tool. *Journal of Coastal Research*, 29: 283-300.

Brander, R.W., 1999. Field observations on the morphodynamic evolution of a low-energy rip current system, *Marine Geology*, 157: 199-217.

Bonneton, P., Bruneau, N., Castelle, B. and Marche, F. 2010. Large-scale vorticity generation due to dissipating waves in the surf zone, *Discrete and Continuous Dynamical Systems - Series B*, 13: 729–738.

Bruneau, N., Bonneton, P., Castelle, B. and Pedreros, R., 2011. Modeling rip current circulation and vorticity in a high-energy meso-macrotidal environment, *Journal of Geophysical Research*, 116, C07026, doi:10.1029/2010JC006693.

Castelle, B., Michallet, H., Marieu, V., Leckler, F., Dubarbier, B., Lambert, A., Berni, C., Bonneton, P., Barthélemy, E. and Bouchette, F., 2010. Laboratory experiment on rip current circulations over a moveable bed : Drifter measurements, *Journal of Geophysical Research*, 115, C12008, doi:10.1029/2010JC006343.

Castelle, B., Michallet, H., Marieu, V. and Bonneton, P., 2011. Surfzone retention in a laboratory rip current, *Journal of Coastal Research*, SI 64 : 50-54.

Castelle, B. and Ruessink, B.G., 2011. Modeling formation and subsequent nonlinear evolution of rip channels: time-varying versus time-invariant wave forcing, *Journal of Geophysical Research*, 116, F04008, doi:10.1029/2011JF001997.

Castelle, B. and Coco, G., in press. Surf zone flushing on embayed beaches. *Geophysical Research Letters*. doi:10.1002/grl.55559

Dalrymple, R.A., 1975. A mechanism for rip current generation on an open coast, *Journal of Geophysical Research*, 80(24), doi:10.1029/JC080i024p03485

Dalrymple, R.A., MacMahan, J.H., Reniers, A.J.H.M. and Nelko, V., 2011. Rip currents, *Annual Review of Fluid Mechanics*, 43: 551–581.

Johnson, D. and Pattiaratchi, C., 2004. Transient rip currents and nearshore circulation on a swell-dominated beach, *Journal of Geophysical Research*, 109(C2), doi: 10.1029/2003JC001798.

Long, J.W. and Ozkan-Haller, H.T., 2005. Offshore controls on nearshore rip currents, *Journal of Geophysical Research*, 110(C2), doi:1 0.1029/2005JC003018.

McCarroll, R.J., Brander, R.W., MacMahan, J.H., Turner, I.L., Reniers, A.J.H.M., Brown, J.A., 2013. RIPSAFE: Rip Current Swimmer and Floater Experiments, Shelly Beach, NSW, Australia, *Journal of Coastal Research*, Special Issue No. 65: 784-789.

MacMahan, J.H., Reniers, A.J.H.M., Thornton, E.B. and Stanton, T.P., 2004a. Infragravity rip current pulsations. *Journal of Geophysical Research*, 109, C01033, doi:10.1029/2003JC002068.

MacMahan, J. H., Reniers, A.J.H.M., Thornton, E.B. and Stanton, T.P., 2004b. Surf zone eddies coupled with rip current morphology, *Journal of Geophysical Research*, 109, C07004, doi:10.1029/2003JC002083.

MacMahan, J.H., Thornton, E.B. and Reniers, A.J.H.M., 2006. Rip current review, *Coastal Engineering*, 53: 191–208.

MacMahan, J.H., Brown, J.W., Brown, J.A., Thronton, E.B., Reniers, A.J.H.M., Stanton, T.P., Henriquez, M., Gallagher, E.L., Morrison, J., Austin, M.J., Scott, T.M. and Senechal, N., 2010. Mean Lagrangian flow behavior on an open coast rip-channeled beach. A new perspective, *Marine Geology*, 1-4: 1-15.

Murray, T., Cartwright, N. and Tomlinson, R., 2013. Video-imaging of transient rip currents on the Gold Coast open beaches, *Journal of Coastal Research*, Special Issue No. 65: 1809-1814.

Reniers, A.J.H.M., MacMahan, J.H., Thornton, E.B., Stanton, E.B., Henriquez, M., Brown, J.W., Brown, J.A., and Gallagher, E.L., 2009. Surfzone retention on a rip-channeled beach, Journal of Geophysical Research, 114, C10010, doi:10.1029/2008JC005153.

Reniers, A.J.H.M., MacMahan, J.H., Beron-Vera, F.J. and Olascoaga, M.J., 2010. Rip-current pulses tied to Lagrangian coherent structures, *Geophysical Research Letters*, 37, L05605, doi:10.1029/2009GL041443.

Roelvink, J.A., Reniers, A.J.H.M., van Dongeren, A.R., van Thiel de Vries, J.S.M., MacCall, R.T. and Lescinski, J., 2009. Modelling storm impacts on beaches, dunes and barrier islands, *Coastal Engineering*, 56: 1133-1152.

Scott, T.M., Russell, P.E., Masselink, G., Austin, M.J., Wills, S. and Wooler, A., 2011. Rip current hazards on large-tidal beaches in the United Kingdom. In: S. Leatherman and J. Fletemeyer (editor), *Rip Currents: Beach Safety, Physical Oceanography, and Wave Modeling*, pp. 225–242.

Short, A.D., 2007. Australian Rip Systems - Friend or Foe, *Journal of Coastal Research*, Special Issue No. 50: 7–11.

Shadden, S.C., Lekien, F. and Mardsen, J.E., 2005. Definition and properties of Lagrangian coherent structures from finite-time Lyapunov exponents in two-dimensional aperiodic flows, *Physica D*, 212: 271–304, doi:10.1016/j.physd.2005.10.007.

Shanks, A.L.S., Morgan, G., MacMahan, J.H. and Reniers, A.J.H.M., 2012. Surf zone physical and morphological regime as determinants of temporal and spatial variation in larval recruitent, *Journal of Experimental Marine Biology and Ecology*, 392: 140–150.